Tectonophysics 623 (2014) 1–13

Contents lists available at ScienceDirect

Tectonophysics

journal homepage: www.elsevier.com/locate/tecto

Constraints for the recent tectonics of the El Salvador Fault Zone, Central America Volcanic Arc, from morphotectonic analysis

Jorge Alonso-Henar [a,b,*], José António Álvarez-Gómez [a], José Jesús Martínez-Díaz [a,c]

[a] Universidad Complutense de Madrid, Geodynamics, Madrid, Spain
[b] CEI Campus Moncloa, UCM–UPM, Madrid, Spain
[c] IGEO, Instituto de Geociencias, UCM–CSIC, Madrid, Spain

ARTICLE INFO

Article history:
Received 18 April 2013
Received in revised form 16 October 2013
Accepted 12 March 2014
Available online 20 March 2014

Keywords:
Active tectonics
Hypsometry
Tectonic geomorphology
Transtension
El Salvador Fault Zone
Strike-slip fault

ABSTRACT

We have used hypsometric analysis to improve our understanding of the current tectonic deformation and structure of El Salvador Fault Zone; a N90°E oriented strike-slip fault zone that extends 150 km through El Salvador, Central America. Our results indicate an important amount of transtensive strain along this fault zone, providing new data to understand the tectonic evolution of the Salvadorian volcanic arc. We have defined kilometric scale tectonic blocks and its relative vertical movements, length of segments with homogeneous vertical motions and lateral relay of active structures. We have identified and quantified slip-rate variations along-strike of the El Triunfo fault within El Salvador Fault Zone, ranging from 4.6 mm/year in its central parts to 1 mm/year towards the tips of the fault. This study supports the hypothesis of a recent rotation in the maximum shortening direction, and the accommodation of the current deformation through the reactivation of pre-existing structures inherited from a previous tectonic regime.

1. Introduction

El Salvador is located in northern Central America, in the western margin of the Caribbean plate. Crossing El Salvador with a N90°E direction, there is a 150 km long right lateral strike-slip fault zone first described by Martínez-Díaz et al. (2004) and named as El Salvador Fault Zone. The southern area of the country is part of the forearc sliver of the Caribbean plate, while the northern part of this country belongs to the Chortís Block (Fig. 1A), a continental block composed by a Paleozoic basement, mesozoic marine sediments and volcanic material associated to the Cocos plate subduction beneath this block (Rogers et al., 2002).

The neotectonic evolution of the Chortís Block region has been studied by many authors at different scales and using several tools. At a regional scale, it has been studied using GPS data, numerical modeling and through seismotectonics and seismologic analysis (i.e. Álvarez-Gómez et al., 2008; Cáceres et al., 2005; Correa-Mora et al., 2009; DeMets et al., 2007; Franco et al., 2012; Guzmán-Speziale, 2001). At a local scale, faulting and tectonics in the Central America Volcanic Arc have been studied through paleoseismology and tectonic geomorphology (Canora et al., 2012; Corti et al., 2005; Ruano et al., 2008). All of these authors conclude the existence of a transtensive regime in the western boundary of the Chortís Block. The transtensive regime along the volcanic arc is driven by the relative eastward drift of the Caribbean plate relative to the North America plate, being the forearc sliver pinned to the North American plate (Álvarez-Gómez et al., 2008). Also, it is important to highlight that there is an important change in scale between the studies done on the Chortís Block at a regional scale and the detailed studies carried out in different segments of the ESFZ. This makes it difficult to compare local observations with the regional morphotectonic features in the area.

For these reasons we consider it necessary to tackle this problem developing an intermediate scale study in order to improve our understanding of the ESFZ, its tectonic behavior and hazard implications. The transtensive regime may be reflected in local tectonic and geomorphological evidences and in the structural and geomorphological characteristics of the ESFZ (Fig. 1B). The analysis of the recent morphotectonics along this fault zone using geomorphological indexes can be useful to address these aspects.

The study of the recent topographic development and the use of geomorphological indexes are adequate tools for the quantification of the active tectonics (Burbank and Anderson, 2001; Keller and Pinter, 2002). At Central America the studies developed using geomorphological indexes are scarce (i.e. Álvarez-Gómez, 2009; Hare and Gardner, 1985; Morell et al., 2012). Previous studies describe a transtensive tectonic regime at the Central America Volcanic Arc in El Salvador (Fig. 1A), which induces relative vertical motions on the faults within El Salvador Fault Zone (i.e. Álvarez-Gómez et al., 2008; Cáceres et al., 2005; Canora et al., in press). We have mainly utilize hypsometry

* Corresponding author at: Facultad de Ciencias Geológicas (Geodinámica), C/José Antonio Novais 12, 28040 Madrid, Spain.
E-mail address: jahenar@geo.ucm.es (J. Alonso-Henar).

http://dx.doi.org/10.1016/j.tecto.2014.03.012
0040-1951/

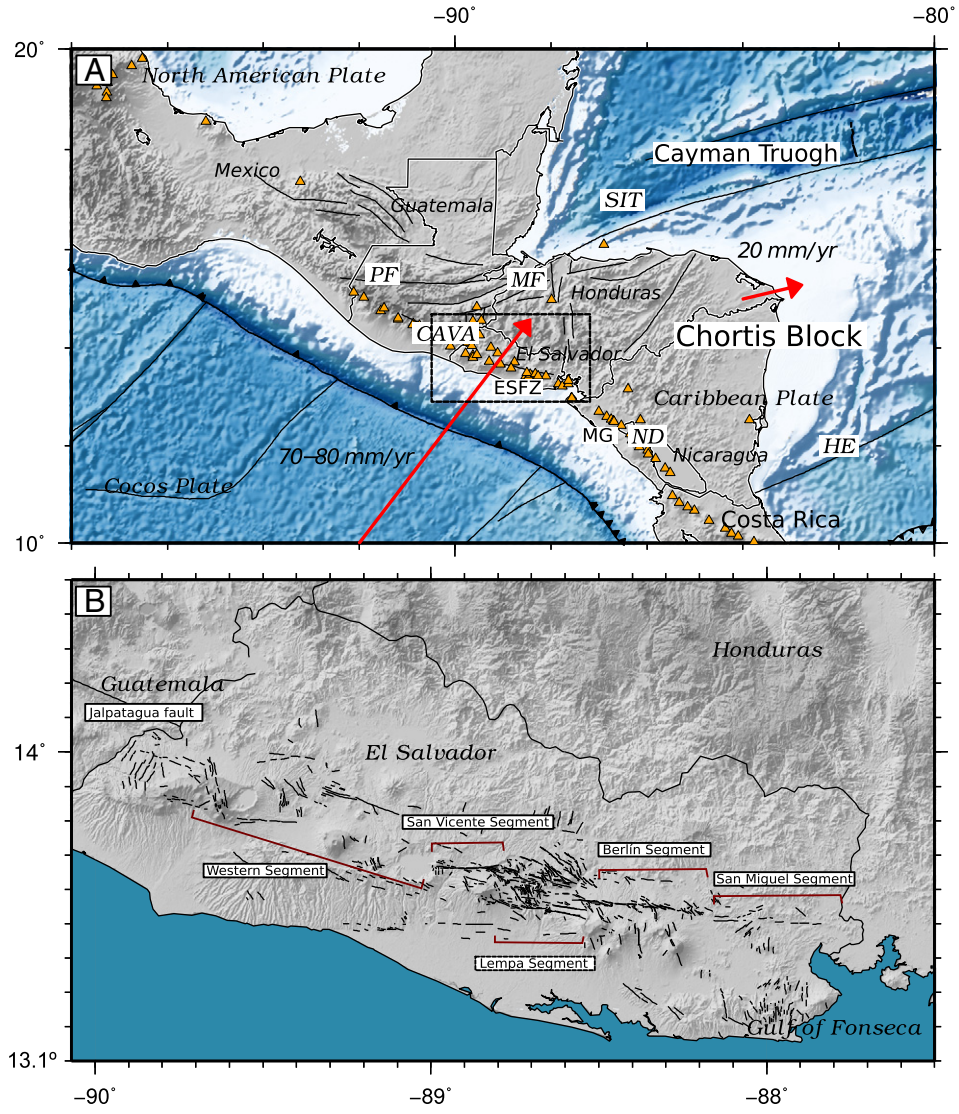

Fig. 1. A: Tectonic setting of northern Central America. Red arrows show relative displacements and its magnitude. Orange triangles show volcanoes from Central America Volcanic Arc. Area enclosed in rectangle is Fig. 1B. Abbreviations are: SIT: Swan Island Transform; MF: Motagua Fault; PF: Polochic Fault; ND: Nicaraguan Depression; HE: Hess scarp; CAVA: Central America Volcanic Arc. B: SRTM image of El Salvador. Black lines are main and secondary active faults, after Canora et al. (2012).

(Strahler, 1952), because the possible dip-slip component in the faults forming ESFZ should be reflected on this index. The relative vertical movements associated to these faults may create differences in the evolution of the adjacent basins. The measuring of the area–altitude relationships of the basins could reflect the relative motions of the hanging and foot walls of the faults (Keller and Pinter, 2002). Up to know, studies in active tectonics in El Salvador have been focused on the strike-slip motion of the ESFZ (i.e. Corti et al., 2005; Martinez-Díaz et al., 2004), but there are no studies focused on the relative vertical motion related to these faults.

In this work we define kilometric scale tectonic blocks and its relative movements to constrain the recent strain distribution along the ESFZ, the length of segments with homogeneous vertical movements and the lateral relay of active structures. The results of this study support the hypothesis of a recent rotation in the maximum shortening direction, and the accommodation of the current deformation along structures formed in a previous tectonic frame. A similar tectonic evolution in Nicaragua as described by Weinberg (1992) is interpreted from the results of this work of El Salvador.

2. Tectonic setting

El Salvador is located in the western margin of the Chortís Block, where a volcanic arc is present (Central America Volcanic Arc), extending from northern Costa Rica to Guatemala. The Central America Volcanic Arc (CAVA) ends abruptly at the Polochic Fault in Guatemala (Fig. 1A). The volcanic arc has been divided into three main zones according to its orientation, the style of its structures and geomorphology (Álvarez-Gómez, 2009). From south to north the main structures within the Central America Volcanic Arc are: The Nicaraguan Depression, from Northern Costa Rica to the eastern Gulf of Fonseca (McBirney and Williams, 1965; van Wik de Vries, 1993), the El Salvador Fault Zone, from western Gulf of Fonseca to approximately El Salvador–Guatemala border (Martínez-Díaz et al., 2004) and the Jalpatagua Fault in Guatemala (Carr, 1976).

The northern boundary of the Chortís block is the Motagua–Polochic–Swan Island transform fault (North boundary of the Caribbean plate), a fault zone with pure left lateral strike-slip motion. The interaction between the Caribbean, North America and Cocos plates results in a

diffuse triple junction at Guatemala, where the deformation is distributed in a broad area (i.e. Authemayou et al., 2011; Guzman-Speziale and Meneses-Rocha, 2000; Guzmán-Speziale et al., 1989; Lyon-Caen et al., 2006; Plafker, 1976). According to Lyon-Caen et al. (2006) and DeMets et al. (2010), the convergence between Cocos and Caribbean plates has a N40ºE trend and a velocity rate of 70–80 mm/year, and the Caribbean plate has a velocity rate of 20 mm/year eastward relative to the North-America plate (Fig. 1A).

The El Salvador Fault Zone is a 150 km long and 20 km wide deformation band within the Salvadorian volcanic arc in the CAVA (Fig. 1B) (Martinez-Díaz et al., 2004). This deformation band is composed of main strike-slip faults trending N90°-100°E, and secondary normal faults trending between N120ºE and N170ºE. The ESFZ continues westward connecting with the Jalpatagua Fault. Eastward ESFZ becomes less clear, disappearing at the Gulf of Fonseca (Fig. 1B).

The ESFZ deforms and offsets Quaternary deposits with a right lateral displacement in its main segments and clearly affects the geomorphology and relief (Fig. 2A) (Corti et al., 2005; Martinez-Díaz et al., 2004). The ESFZ offsets Quaternary ignimbrites and pyroclastic flows of Tierra Blanca Joven and Cuscatlán Formations (Fig. 2B). Horizontal offsets up to 200 m of Holocene deposits and drainage network have been described by Corti et al. (2005) and Canora et al. (2012).

Five segments have been proposed for the whole fault zone, from the Jalpatagua Fault to the Gulf of Fonseca (Canora et al., 2010). From west to east these segments are: Western segment, San Vicente Segment, Lempa Segment, Berlin Segment and San Miguel Segment (Fig. 1B). Here we renamed the Lempa Segment as Lempa Inter-Segment, because this is an area of distributed deformation with normal and strike-slip faults connecting two well constrained deformation zones (San Vicente and Berlin segments).

This study is focused on the San Vicente, Lempa and Berlin segments, and specifically on its interactions (Fig. 2A). The main faults of the segments are: The San Vicente fault in the San Vicente Segment; El Triunfo fault in the Berlin Segment and Lempa fault in the Lempa inter-segment. The studied area has a very clear geomorphological expression of the recent fault activity. The Lempa inter-segment, located between San Vicente and Berlin segments, is especially interesting because the deformation is distributed in a large set of N120°-170°E trending normal faults that seem to connect both segments; potentially increasing the maximum rupture length capability of the ESFZ and the seismic hazard, as stated in Canora et al. (2012). Seismotectonic and paleoseismological data reveal a large seismic potential in ESFZ, in fact the San Vicente segment has been the source of the February 13th, 2001 earthquake (Canora et al., 2010, 2012; Martínez-Díaz et al., 2004). In the Berlin Segment the data are scarcer, only Corti et al. (2005) presented a detailed analysis of the activity of this segment based on the mapping of the fluvial network and ignimbrites affected by the recent fault activity. They concluded that ESFZ has a slip rate of ~11 mm/year from the late Pleistocene–Holocene strike-slip motion of the fault.

3. Regional morphometric analysis

In order to extract information about the fault interactions and the lateral distribution of the vertical displacements along the faults within the ESFZ, we have carried out a morphometric analysis using topographic data. This analysis includes the calculation of geomorphological indexes such as hypsometric curves, hypsometric integral and the analysis of the basins' orientations.

The whole study is developed from a 10 m resolution Digital Terrain Model (DTM), supplied by the MARN (Ministerio de Medio Ambiente y Recursos Naturales de El Salvador) obtained from the digitalization of 1:25,000 topographical maps. We used Geographical Information System free software tools (GRASS, GDAL and Qgis), as well as scripts in Bash environment using AWK and GMT (Wessel and Smith, 1991) for data processing and graphic representation.

3.1. The hypsometric curve and the hypsometric integral

The hypsometric curve describes the elevation distribution of the relief in a specific area, in a scale which may range from a basin to the whole planet (Keller and Pinter, 2002). It represents the area distribution existing above a determined elevation range related to the total area (Strahler, 1952). It is usual to represent the area (a) and elevation (h) normalized to one (i.e.: Cheng et al., 2012; Keller and Pinter, 2002; Perez-Peña et al., 2010; Walcott and Summerfield, 2008), which allows an easy comparison between different hypsometric curves in a specific study. The shape of the hypsometric curves may give us information about the relative evolution stage of the fluvial basin development. Thereby, a convex hypsometric curve indicates a "youthful" stage of the basin; S shape hypsometric curve indicates an intermediate stage of the evolution (an area moderately eroded); and concave curves indicate "old-mature" basins (Keller and Pinter, 2002). Hypsometric integrals values (H_i) have also been calculated. H_i is defined as the area under the hypsometric curve, which is equivalent to the equation of Pike and Wilson (1971): H_i = (mean elevation − minimum elevation)/(maximum elevation − minimum elevation). Therefore, values of H_i near 1 mean "youthful" stage of the basin and values of H_i near 0 mean "old-mature" stage of the basins.

Strahler (1952) applies the hypsometric analysis to drainage basins and the manner in which the mass is distributed within it. He related the area–altitude relationship with the stage of the cycle of erosion. In some cases it is possible to relate the stage of the cycle with the tectonic activity. It is because the cycle of erosion could be interrupted by an uplift episode and rejuvenates the drainage basin (Keller and Pinter, 2002). Hence, the raised areas are in the early stages of erosion (concave hypsometric curves and H_i values near 1), and the sunk areas in mature-old stages of the cycle (convex hypsometric curves and H_i values near 0).

According to Strahler (1952), the hypsometric curve is independent of the basin size. On the other hand, Cheng et al. (2012) concluded that variations could exist for the steady-state topography in result of the hypsometric analysis related to the basin order and size. To avoid scale problems, each analysis has been made using areas of similar size. In order to identify the basins in an objective way and at a homogeneous scale, we have used GRASS basin identification tools on the DTM 10 m resolution.

3.2. Hypsometric integral mapping

Following the criteria described above a hypsometric integral value map has been done (Fig. 2C). To make this map, we carried out a topographic analysis following the equation of Pike and Wilson (1971). This map has been done cutting the DTM with a moving window of constant area. We calculated the H_i value in each cell, providing xyz values for each calculation (Longitude, Latitude and H_i). We have used a cell area of 0.02 × 0.02° (approximately 2000 × 2000 m at latitude 13°) and a window step of 0.004° (approximately 400 m).

In the H_i map (Fig. 2C), we have represented the hypsometric integral values (from 0 to 1). The results of the hypsometric integral follow a normal distribution with the mean, mode and median close to each other (0.429, 0.45 and 0.438 respectively). The graphic representation has been done following a color code, where the red shades show the values higher than the mode (>0.45) and the blue shades show the values lower than the mode (<0.45). Hereby, it is possible to observe gradients separating domains with different integral values.

To avoid possible erroneous interpretations due to potential gradients associated with lithological heterogeneities, we compare this map with the geological map in Fig. 2B. We will discuss this below in detail.

3.3. Hypsometric zonification

In the map of Fig. 2C we observe patterns, analogies and differences between different areas. We have distinguished several kilometric-scale

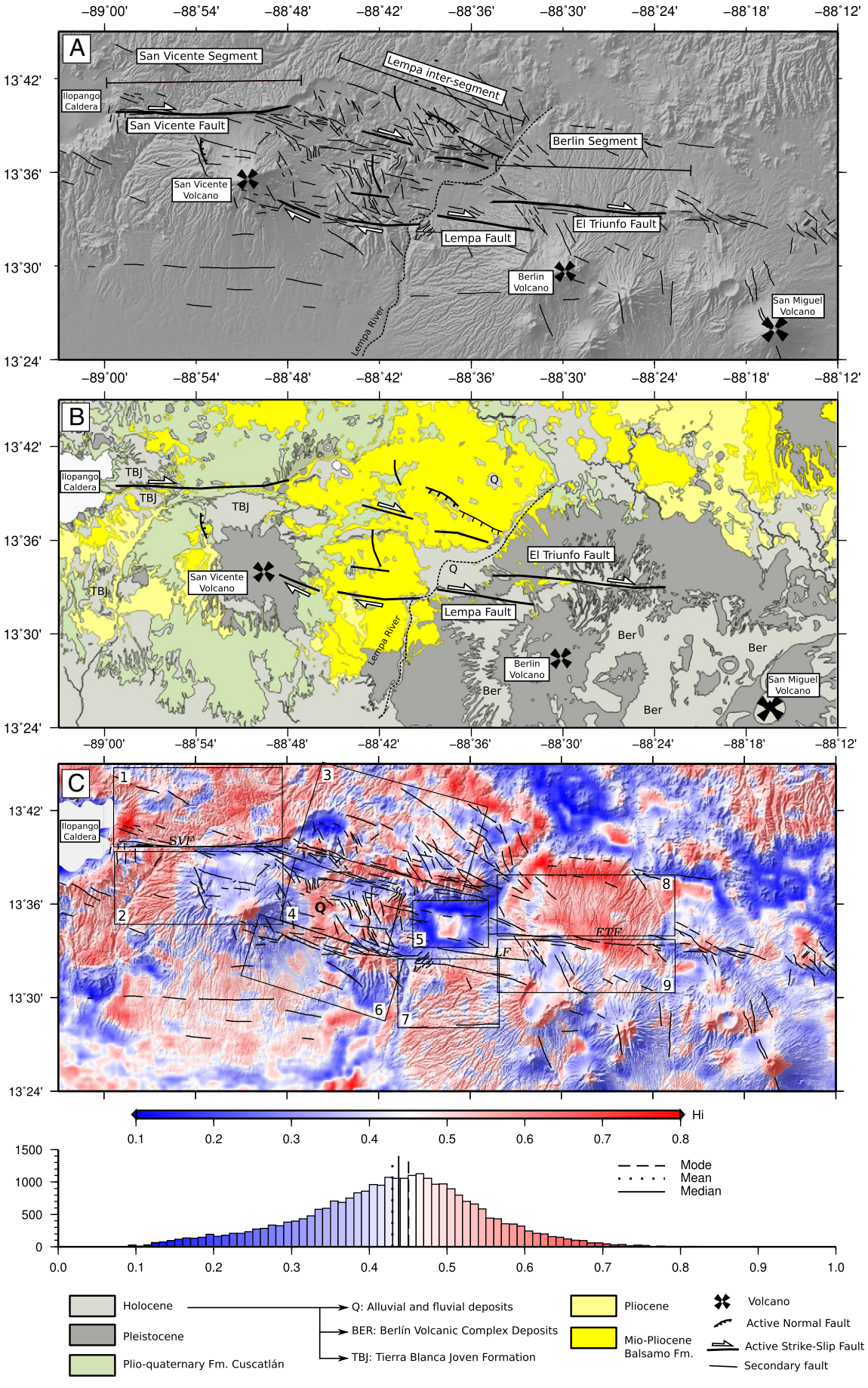
A
San Vicente Segment
Lempa inter-segment
Ilopango Caldera
San Vicente Fault
Berlin Segment
San Vicente Volcano
El Triunfo Fault
Lempa Fault
Berlin Volcano
San Miguel Volcano
Lempa River
B
TBJ
Q
Ber
C
SVF
ETF
LF
Hi
Mode
Mean
Median
Holocene
Pleistocene
Plio-quaternary Fm. Cuscatlán
Q: Alluvial and fluvial deposits
BER: Berlín Volcanic Complex Deposits
TBJ: Tierra Blanca Joven Formation
Pliocene
Mio-Pliocene Balsamo Fm.
Volcano
Active Normal Fault
Active Strike-Slip Fault
Secondary fault

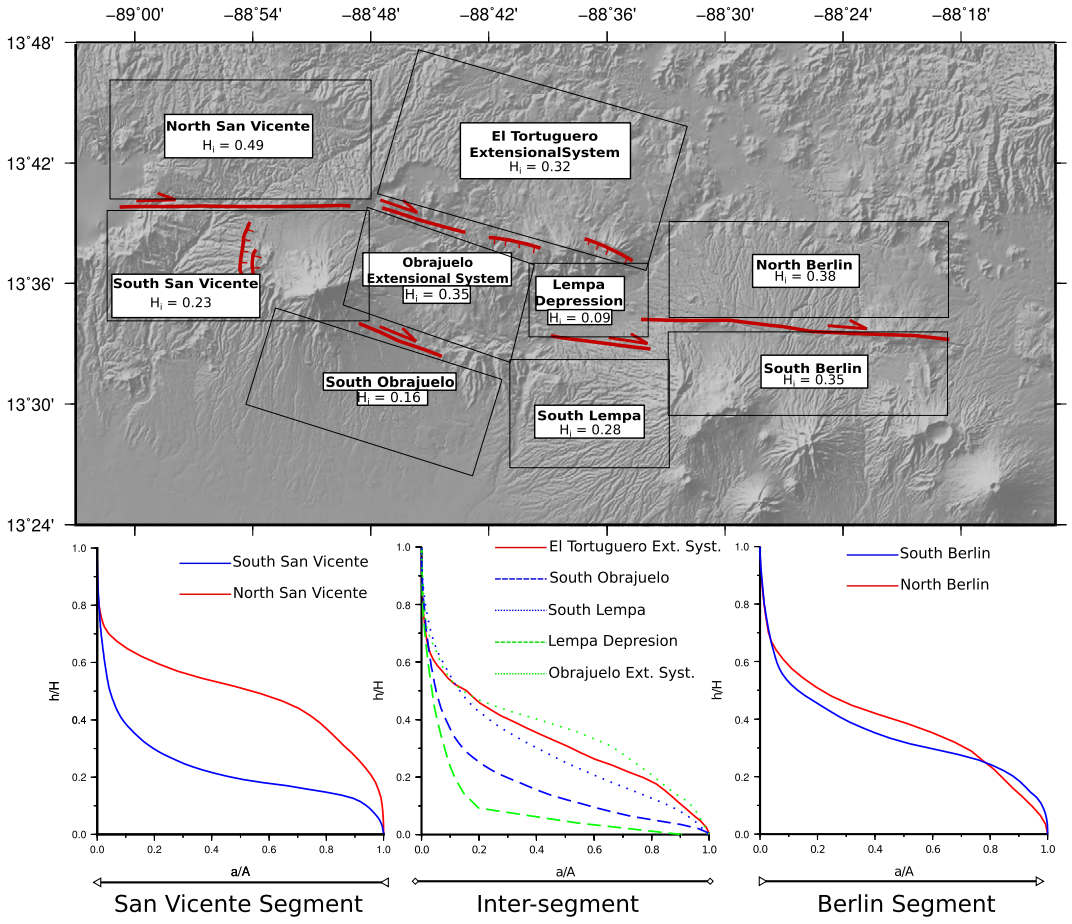

Fig. 3. Main blocks and its hypsometric integral value (H_i) and hypsometric curves. Red lines are the main faults.

blocks that present similar patterns in the H_i value distribution (Fig. 3). We have calculated the hypsometric curve for each block to characterize potential relative movements between them. We have defined nine blocks, five of them are located in the inter-segment zone.

3.3.1. San Vicente blocks

We have defined two blocks in the western part of the study area. A northern block (North San Vicente, number 1 in Fig. 2C), with predominant high values of H_i, and a southern block (South San Vicente, number 2 in Fig. 2C), with lower values of H_i (Fig. 2C). Attending to the geometry of the hypsometric curve for the whole blocks of the San Vicente area (Fig. 3), we can see a significant difference between both of them. The hypsometric curve of the North San Vicente block is convex ($H_i = 0.49$), while the one in the South San Vicente block is concave ($H_i = 0.23$) (Fig. 3).

3.3.2. Berlin blocks

There is a predominance of higher values of H_i to the north of the El Triunfo Fault, therefore we have distinguished a block north of the fault and another one to the south of the fault. The results of this block show S-shaped hypsometric curves for both described blocks, with little differences between them, having values of the Northern and Southern blocks of 0.38 and 0.35 respectively (numbers 8 and 9 in Fig. 2C).

3.3.3. Lempa inter-segment blocks

In the Lempa inter-segment, the differences between H_i values are not very well constrained (Fig. 2C). Nevertheless, we have identified five blocks with different patterns of the values distribution in the inter-segment area (Figs. 2C and 3). One of them is located in the northern part: El Tortuguero extensional system (number 3 in Fig. 2C); two of them are in the central part: Obrajuelo extensional system and Lempa depression (numbers 4 and 5 in Fig. 2C); and finally, two in the southern part, separated by the Lempa river (numbers 6 and 7 in Fig. 2C): South Obrajuelo and South Lempa.

The extensional systems of Obrajuelo and El Tortuguero are highly fractured by secondary normal faults. Both areas have similar shapes of the hypsometric curve and similar H_i values (Fig. 3).

El Tortuguero extensional system is lithologically homogeneous (Mio-Pliocene lavas of Bálsamo Formation), and it is highly fractured by N120°-150°E trending secondary normal faults, resulting in a horst and graben structure, causing the collapse of the volcanoes bounding to the north of the Lempa Depression (Fig. 3). The gradients of Hi values

Fig. 2. A: Interpreted structures of the study area overlaid onto 10 m resolution DTM derived from 1:25,000 topographic map. B: Geological map (Bosse et al., 1978). C. Shaded hypsometric integral map and histogram of the analysis results. SVF: San Vicente fault; LF: Lempa Fault; ETF: El Triunfo Fault. Secondary faults interpreted by Canora et al. (2012). Rectangles are the distinguished blocks: 1: North San Vicente; 2 South San Vicente; 3: El Tortuguero Extensional System; 4: Obrajuelo extensional System; 5: Lempa Depression; 6: South Obrajuelo; 7: South Lempa; 8: North Berlin; 9: South Berlin. Q marked anomaly explained in the text.

on the map are arranged along the N120°–150° direction corresponding with the secondary normal faults trending (Fig. 2C).

Obrajuelo extensional system is composed of penetrative sets of N180°E trending and N120°E normal faults that produce the collapse of volcanoes, as in El Tortuguero extensional system. There is an anomaly (high values of H_i, marked with a Q in Fig. 2C), which corresponds to Plio-Quaternary deposits of Cuscatlan formation. The remaining area of Obrajuelo Extensional System is lithologically homogeneous.

The Lempa depression zone presents the most concave hypsometric curve and the lowest values of H_i, typical of the "old" and stable basins (Strahler, 1952, Fig. 3). In the central part of the depression, there is a positive gradient to higher values of H_i (Fig. 2C), which are bounded on the north by a possible N90°E trending fault, with smooth geomorphological expression, affecting Quaternary deposits of Lempa fluvial system (Fig. 4) and defined by Canora et al. (2012).

The blocks defined at the southern part of the inter-segment zone (South Obrajuelo and South Lempa Blocks, 6 and 7 in Fig. 2C) are bounded by the contact between Mio-Pliocene deposits of Balsamo Formation and Holocene deposits of the Berlin volcanic complex. The pattern of the distribution of H_i values is different between both blocks (Fig. 2C). These blocks are the southern limit of the transtensional area and they are less fractured than the ones defined before. The South Obrajuelo block presents a concave geometry of the hypsometric curve and it is composed mainly by Mio-Pliocene deposits. The South Lempa blocks composed of Holocene deposits of the Berlin volcanic complex also show a concave hypsometric curve but with more predominance of higher altitudes that represents an intermediate stage of the evolution of the topography (Fig. 3).

4. Local morphometric analysis

Here we present the results of the local analysis carried out in the drainage basins northward and southward of the main faults (San Vicente, Lempa and El Triunfo Faults, Fig. 5 and Table 1) and combine the results with the local variations identified in the H_i spatial distribution. We have carried out a detailed analysis with the aims of identifying lateral variations of the vertical slip and individualize segments. We have considered small drainage basins and we calculated the hypsometric curve and integral of each one.

4.1. San Vicente fault

Attending to the geometry of the hypsometric curve for the individualized drainage basins of the surrounding areas of the San Vicente fault (Fig. 5), we can see that most of the northern basins (red in Fig. 5) have convex geometry; while most of southern basins (blue at Fig. 5) have concave geometry. There are some basins that are not following this pattern, these are those situated at the western part of the fault (basins 13 and 14 in Fig. 5, Table 1), near the Ilopango Caldera. This observation will be discussed below.

4.2. El Triunfo and Lempa faults

A further detailed study has been done in the El Triunfo and Lempa Faults. In these areas there are strong variations in the distribution of the H_i values (Fig. 2C). In this area, topographical effects prior to the recent tectonic activity could also be discarded (paleo-topography), because the topography has been blanked by the recent volcanic activity of the Berlin volcanic complex. The H_i values northward of the El Triunfo fault are higher than 0.6, while southward of the fault the values are lower than 0.4. This is the highest difference along the ESFZ. These facts make this area a good place to delve into the morphotectonic study.

The Lempa Fault has been studied together with the El Triunfo Fault due to its proximity. In this area the hypsometric values between the northern and southern basins have no significant differences. In Fig. 5B the hypsometric curves of the basins from 33 to 47 are represented. Blue lines are the southern basins and red lines are northern basins.

Hypsometric curves of the surrounding basins of the El Triunfo Fault normalized to one, have been represented in Fig. 5C. The curves represented in red lines are the hypsometric curves of the basins situated northward of the El Triunfo Fault (basins from 24 to 32 in the map of Fig. 5 and Table 1). They show S shapes and convex geometry. Hypsometric curves represented in blue lines are for the southern basins of the El Triunfo Fault (basins from 48 to 59 in the map of Fig. 5 and Table 1), and they have concave geometries (Fig. 5C).

5. Interpretation and discussion

In spite of the fact that the faults of ESFZ have a predominant strike-slip component, the hypsometric analyses reveal that the normal component of the main faults is significant, at least in the studied segments.

5.1. Lithological influence in the results of the analyses

Previous to any interpretation about uplift and relative movements of the blocks defined, it is mandatory to dismiss possible non-tectonic effects on the topography and thereby to the area–altitude relationship.

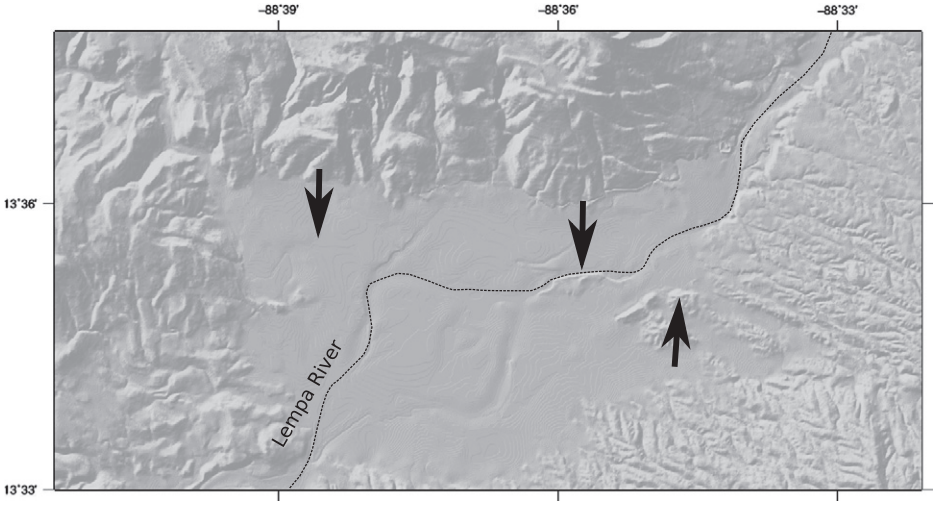

Fig. 4. Lempa depression detail. The location of this figure corresponds to Lempa Depresion block described in Fig. 3. Arrows are indicating an inferred fault.

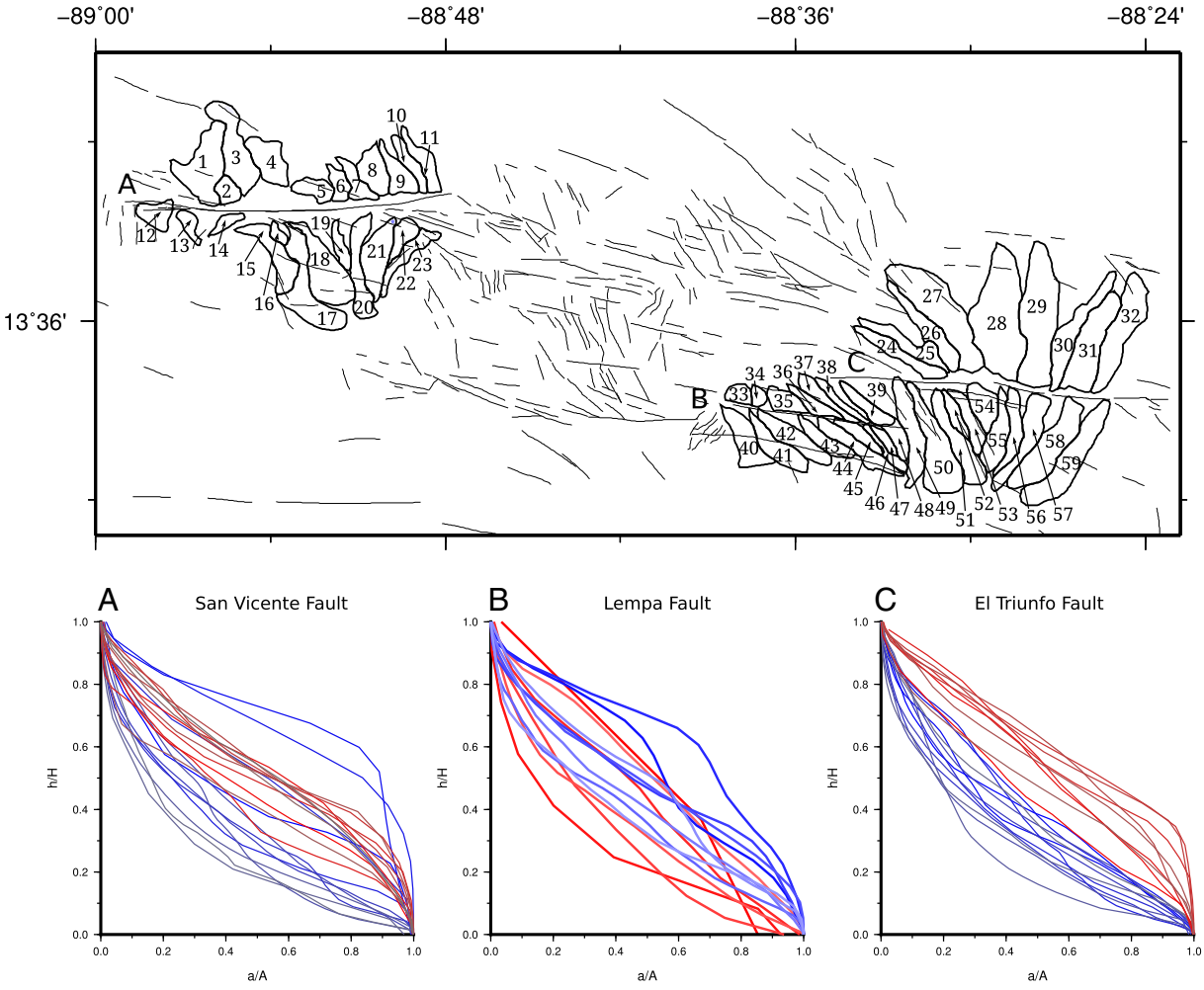

Fig. 5. Map showing the analyzed basins. Basin numbers of Table 1. A, B and C are showing the positions of San Vicente, Lempa and El Triunfo Faults respectively on the map. A: Hypsometric curves of the San Vicente segment surrounding basins. B: Hypsometric curves of the Lempa Fault surrounding basins. C: Hypsometric curves of the El Triunfo Fault surrounding basins. Red lines are north basins. Blue lines are south basins.

There are some gradients in the results of the H_i map that we have interpreted as a lithological effect in the hypsometric results.

Comparing the H_i value map and the geological map we can see that there are some hypsometric anomalies which are coincident with tephra deposits, especially with the tephras of Tierra Blanca Joven Formation (TBJ; Hart, 1981, 1983) and the pyroclastic flows of the Cuscatlán Formation (Plio-quaternary) (Fig. 2B and C). These deposits cover and "rejuvenate" the topography. The regions with these recent deposits are in an early-state of erosion which increases the area of high elevations in specific areas, and induces a larger value of the H_i.

This effect is clearly observed in the boundaries of Ilopango Caldera, where higher values of H_i correspond to TBJ deposits. Lithological effects are also observed south of the San Vicente Volcano, where high values of H_i are coincident with Plio-Quaternary deposits of Cuscatlán Formations and TBJ Formation. However, south of San Vicente fault there are low values of H_i ($H_i < 0.45$) in areas covered by TBJ deposits. These results can be interpreted as a consequence of the dip-slip movements of this fault (the normal component of the fault). In this case the TBJ deposition could be smoothing the differences between both walls of the fault due to tectonic movements, resulting in higher values of H_i than expected if there were no TBJ deposits. The results of the local analysis in this fault also show this effect.

The Berlin Formation is also a very young deposit, but it covers the topography in a homogeneous way, so we cannot see clearly any influence in the results of the analysis. In fact, there are gradients of the H_i value in regions with this lithology (Fig. 2 B and C). We relate these gradients with tectonic processes.

5.2. Vertical movements of the tectonic blocks

Attending to the differences of the hypsometric curves and integrals for the blocks defined in Chapter 3.3 (Fig. 3), and taking into account that the results could be conditioned by the lithology, we propose the relative movements of the blocks.

We have interpreted an important uplift of the North San Vicente block relative to the South San Vicente block. Despite the possible influence of the lithology, the differences in the shape of the hypsometric curve and the H_i values are really clear (Fig. 3). The S-shape of the northern block indicates a "mature" stage of the topography, while the concave shape of the southern block indicates an "older" stage of the topography.

According to the hypsometric curve of the North Berlin and South Berlin blocks, we do not see significant differences between them. In this case the lithology is homogeneous in both blocks and we can assume that these differences are related with tectonic movements. Both curves are S-shaped, but there is a predominance of higher altitudes in the North Berlin block. We interpret a relative uplift of the northern block, but it is much lower than the difference between north San Vicente and South San Vicente blocks (Fig. 3).

Table 1
Hypsometric integral value of the analyzed basins. Numbers of the basin in the map of Fig. 7. SV: San Vicente fault; L: Lempa fault; ET: El Triunfo fault. (S): Southern fault; (N): Northern fault and H_i: Hypsometric integral.

Basin Number	Segment	Hi
1	SV (N)	0.45
2	SV (N)	0.52
3	SV (N)	0.41
4	SV (N)	0.5
5	SV (N)	0.55
6	SV (N)	0.54
7	SV (N)	0.54
8	SV (N)	0.53
9	SV (N)	0.41
10	SV (N)	0.51
11	SV (N)	0.53
12	SV (S)	0.44
13	SV (S)	0.69
14	SV (S)	0.67
15	SV (S)	0.33
16	SV (S)	0.5
17	SV (S)	0.33
18	SV (S)	0.34
19	SV (S)	0.38
20	SV (S)	0.32
21	SV (S)	0.28
22	SV (S)	0.24
23	SV (S)	0.26
24	ET (N)	0.44
25	ET (N)	0.53
26	ET (N)	0.56
27	ET (N)	0.58
28	ET (N)	0.62
29	ET (N)	0.62
30	ET (N)	0.59
31	ET (N)	0.55
32	ET (N)	0.48
33	L (N)	0.29
34	L (N)	0.45
35	L (N)	0.28
36	L (N)	0.13
37	L (N)	0.3
38	L (N)	0.33
39	L (N)	0.5
40	L (S)	0.54
41	L (S)	0.62
42	L (S)	0.49
43	L (S)	0.49
44	L (S)	0.36
45	L (S)	0.42
46	L (S)	0.47
47	L (S)	0.37
48	ET (S) L(S)	0.39
49	ET (S)	0.37
50	ET (S)	0.42
51	ET (S)	0.38
52	ET (S)	0.33
53	ET (S)	0.3
54	ET (S)	0.34
55	ET (S)	0.39
56	ET (S)	0.29
57	ET (S)	0.27
58	ET (S)	0.31
59	ET (S)	0.39

In the inter-segment zone the deformation is not well constrained. The extensional systems of El Tortuguero and Obrajuelo have a similar hypsometric curve. There are some deposits from Cuscatlan formation that could have influenced the results, but the lithology could be considered homogeneous along the block. We think that the results are so similar because both systems have equivalent fracturing style and a strong influence of monogenetic volcanoes that are scattered along both areas, conditioning the topography and therefore the results of the analysis.

The South Obrajuelo and South Lempa blocks are bounded by the Lempa River whereas the South Lempa Block is mostly composed of Holocene and Pleistocene deposits from the Berlín Volcanic Complex and the South Obrajuelo Block is mainly composed of Mio-Pliocene rocks of the Bálsamo Formation. We have not identified evidences of tectonic activity between these blocks and they are not much fractured. However, there are some differences in the hypsometric curves that could be explained by lithological heterogeneities

The lowest values of H_i and the most concave hypsometric curve are in the Lempa Depression. The positive gradient of H_i values in the middle of the block is interpreted as a consequence of the activity of a fault crossing the depression (Fig. 4) as described by Canora et al. (2012). Despite the low expression on the relief, the strong gradient of H_i values supports the existence of this fault and its recent activity.

The Lempa block is bounded by normal faults, and we interpret that it is forming the area of maximum subsidence of the pull-apart basin. This is also consistent with some interpretations of Corti et al. (2005) and Agostini et al. (2006).

5.3. Fault slip variation along-strike

A structural segment of a fault can be described as a section of the fault bounded by fault branches, or intersections with other faults, folds, or cross structures (Scholz, 2002, Chapter 3). The existence of a segment in a fault zone implies a distinctive seismic behavior. This means that it acts as an individual fault interacting with adjacent segments. Theoretically, the medium to long-term net slip along a fault segment varies along the fault plane. This behavior, especially in active faults affecting Quaternary materials, should be reflected in topography.

Usually, these variations in the displacement along the faults affect the strike slip and the dip slip components. If the normal component of these faults is enough, this lateral variation should be reflected in the results of the hypsometric analysis. According to theoretical models, maximum accumulated long-term displacements occur in the central part of the faults and decrease gradually towards the tip points (i.e. Cowie and Roberts, 2001; Ferril and Morris, 2001; Scholz, 2002; Walsh and Watterson, 1989). Hence, in central parts, differences in hypsometric curves between the hanging wall block and the foot wall block should be higher than at the tip points of the fault, where hypsometric curves should tend to be equal (Fig. 6).

In order to visualize these lateral variations, we have done profiles along the Lempa, San Vicente and El Triunfo faults representing values of H_i of northern basins (red circles) and southern basins (blue circles) (Fig. 7). To compare their trends we fitted quadratic polynomial regressions, shown as red and blue lines respectively. This regression should fit well the surface displacement of a theoretical elliptical fault rupture, although higher order polynomials could also be used. In addition we have also represented the elevation difference between northern and southern blocks of each fault along the profiles (Fig. 7).

Profile A in Fig. 7 is along San Vicente fault (basins from 1 to 23 in Table 1 and Fig. 7). In the western part of the profile the value distribution and the variations between the northern and southern values are not following a clear pattern. The highest difference between them is in the eastern part. The highest scarp is also situated also in the eastern part (at the length of 20 km, x axis). It does not correspond with the idealized model of Fig. 6, and the fit is not suitable for any side of the fault. We interpret that these high values of the scarp and the differences of H_i are not related with the recent activity of this segment. It could be related with structures inherited from a previous tectonic phase as we discuss below.

Profile B in Fig. 7 has been done along the Lempa fault. The hypsometric integral values of the southern basins are higher than the hypsometric values of the northern basins (Fig. 7, basins from 33 to 47, and Table 1). The differences between the northern and southern H_i values are decreasing from km 6 of the x axis of the profile towards the eastern tip of the profile (km 12).

Profile C in Fig. 7 is along the El Triunfo Fault. In this profile the maximum difference between H_i values is observed in the central part of the

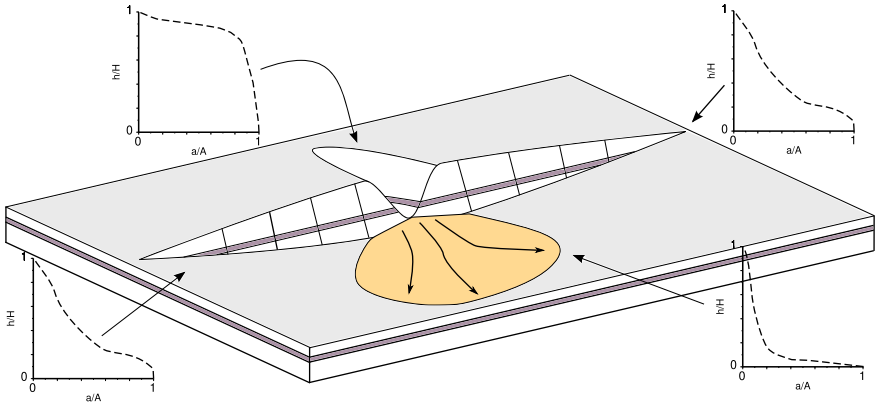

Fig. 6. Idealized behavior of a fault and the expected results of the hypsometric curves.

fault, at km 12 of the profile, from $H_i = 0.62$ in the north to $H_i = 0.38$ in the south. These differences clearly decrease towards the tips of the fault, being non-existent at the tips (Fig. 7 profile C). The fit of the northern values is the best one of all the profiles.

At the El Triunfo Fault, the basin orientations provide important information due to the drainage radial pattern related to the Berlin Volcano (Figs. 2 and 8). We have measured the angle formed by the basins' axis with the fault trace in order to describe the horizontal component of the movement of this fault (Fig. 8). The radial pattern of the drainage basins is the same northward and southward of the El Triunfo Fault. The fault activity produces lateral variations in the orientations and position of the basins. We have represented the basin axes orientation values in Fig. 8. We can see that there are differences up to 30° at km 4 and up to 40° at km 11. The regression shows that the differences are higher in the central part of the fault and they decrease towards the tips. Although, in the eastern part of the fault, the fan pattern of the basins axis became unclear and it is smoothing the results.

We have measure the possible offset of the basins assuming that the basins with the same axis orientation were connected when they were formed. The result shows the greatest offsets in the central-western part of the fault (kms 5 to 12), and the smallest are in the tips (Fig. 8). This drainage network is formed on Pleistocene basaltic lavas from the Berlin volcanic complex and although the age is not well constrained, Bosse et al. (1978) dated them with an age of 1.4 Ma. If we assume that the drainage network formation is contemporaneous with the last basaltic lava extrusion, then we can estimate the horizontal slip-rate of the fault. From the offsets in the basin axes orientation (Fig. 8), we have calculated a minimum slip-rate for El Triunfo fault. The results, from west to east are: 0.75 mm/year, 4.2 mm/year, 4.83 mm/year, 4.79 mm/year, 1.4 mm/year, 1.7 mm/year and 1.4 mm/year (Fig. 8). The fault displacement (D) variation along-strike and the corresponding slip-rate (SR), assuming the age of 1.4 Ma given by Bosse et al. (1978), are also shown in Fig. 8. In this plot, it is clearly seen how the fault slip decreases form km 6 towards the tips of the fault. The slip-rate is highest in km 6 with a value of 4.6 mm/year.

If we assume that 100% of the differences of the H_i value and the differences in the basin orientations are due to the fault activity, we can interpret that the El Triunfo Fault is following an idealized model along a fault displacement distribution. The maximum displacements are observed in the central-western parts of the fault and they decrease towards the tip points.

If we analyze the profiles of Lempa and El Triunfo faults together we can observe a relationship between both. From km 6.5 to the eastern end of the Lempa fault the H_i differences between the north and south basins decrease, while in the El Triunfo Fault increase eastward during the first 10 km (Fig. 7 profiles B and C, overlap zone). We interpreted that there is a deformation relay between the Lempa and El Triunfo overlapping faults that produce an accommodation zone between these faults (Figs. 7 and 9). Westward, Lempa fault absorbs much of the deformation, where H_i differences are higher (Fig. 7 profile B). Eastward, the slip of the Lempa fault decreases since the El Triunfo fault is absorbing much of the deformation. The increase of the H_i value differences in El Triunfo Fault is coincident with the decrease of the H_i value differences in Lempa fault and the overlap zone. An interpretation of this zone as two antithetic faults with normal component but with predominant strike-slip movement and an accommodation zone between both faults as showed in Fig. 9, is consistent with the morphometric results.

5.4. Tectonic evolution

In areas of ESFZ where deformation is accommodated in a narrow shear zone (El Triunfo and San Vicente faults), there exists a clear uplift of the northern block relative to the southern blocks (Fig. 3). The differences between the northern and southern hypsometric curves on these faults are higher in the San Vicente fault than in the El Triunfo Fault. The results of the San Vicente segment analysis do not show a clear pattern in the lateral distribution of Hi differences, and it presents a huge fault scarp in the eastern part of the fault (Fig. 7 profile A). These observations could be explained by three hypotheses: a) a high uplift (large dip-slip movement of the fault) in San Vicente segment of the ESFZ; b) a greater influence of lithology; and c) the existence of inherited structures and associated relief.

Canora et al. (2010, 2012) conclude that the Holocene movement of San Vicente fault is almost pure strike-slip, throughout its seismotectonic and paleoseismological analyses. So we think that the Holocene dip-slip movement of this fault it is not enough to generate the differences seen in the hypsometric results and it does not satisfy all the observations.

We think that the lithological effect, as we have explained in the section specifically focused in this issue, is smoothing the differences between the northern and southern curves of the San Vicente blocks, and neither satisfies all the observation. So we delve in the third option below: the existence of inherited structures and associated relief.

Weinberg (1992) described a neotectonic evolution in western Nicaragua dominated by three different deformation phases from Miocene to Holocene, and thereby two changes in the stress tensor. During the first deformation phase (Miocene–Low Pliocene) dip angle of the subducting plate (Cocos plate) is low and it is coupled, during this stage there is a maximum shortening direction NE–SW, and it generated a folding oriented NW–SE. Then a roll-back produced a rotation of the stresses. This roll-back caused the migration of the volcanic arc southwestward to its current position. During this phase an extensional regime generated the highly asymmetrical half-graben of Nicaragua

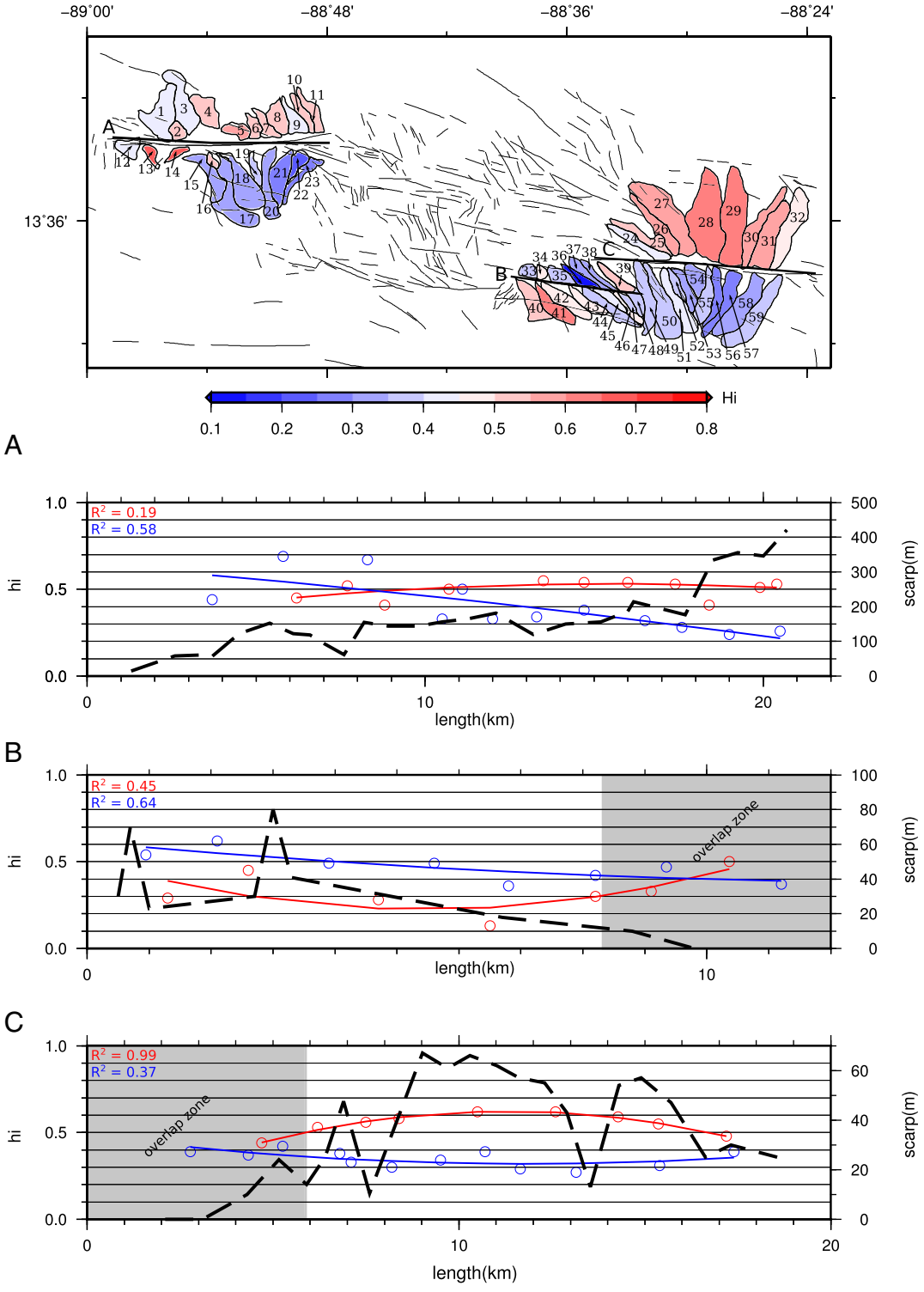

Fig. 7. Map showing the analyzed basins. Basin numbers of Table 1. Lines A, B and C are the profiles 7A, 7B and 7C, coincident with San Vicente, Lempa and El Triunfo faults respectively. Profiles A, B and C are representing H_i values of each basin along the fault. Red circles are the H_i value of each north basin of the fault area. Blue circles are the H_i value of each south basin of the fault area. Red and blue lines are the trend of red and blue circles respectively. Dashed black line is the scarp profile along the fault.

bounded to the southwest by NW–SE, oblique-slip normal faults (Funk et al., 2009). The second rotation occurred during middle Pleistocene to Holocene. This change, caused a maximum horizontal shortening direction rotation from N130°E to the current N–S, forming the Managua Graben (Weinberg, 1992, Fig. 1A).

At El Salvador, the volcanic chain has also migrated southward from the Miocene to its current position. This migration could be also related to the Cocos plate roll-back during late Pliocene–Pleistocene (Weinberg, 1992). This tectonic context could develop E–W dip-slip normal faults similar to the normal faults driving the Nicaraguan half-graben.

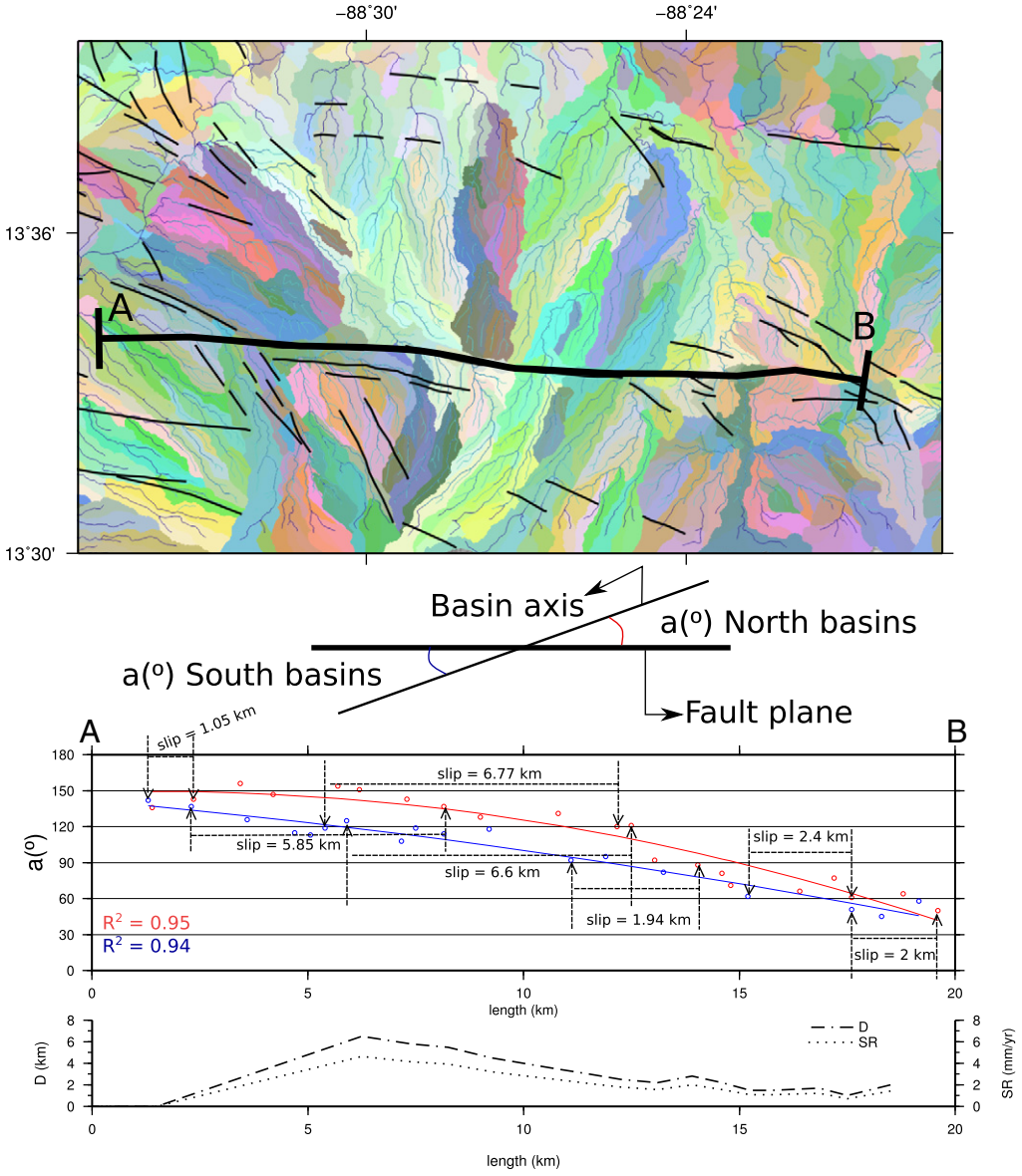

Fig. 8. Map showing the basins of the El Triunfo Fault area. Line A–B is the profile position. Profile showing the differences of the basins' orientation along the fault. Red circles are the orientation of each north basin of the fault area. Blue circles are the orientation of each south basin of the fault area. Red and blue lines are the trend of red and blue circles respectively.

The current tectonic regime reactivated those normal faults as transtensional strike-slip faults and the deformation could be concentrated on them (Canora et al., 2012). This explain the anomalies on the results of the San Vicente Segment and the abrupt scarp in that fault (Fig. 7 profile A, dashed black line), if we interpret the San Vicente fault as a formed dip-slip fault reactivated.

6. Conclusions

This study reveals dip-slip movements in some faults of ESFZ, and lateral changes of the dip-slip and the strike-slip components. The results from our analysis are consistent with some previous results describing a transtensional regime in ESFZ (i.e. Álvarez-Gómez et al., 2008; Cáceres et al., 2005; Canora et al., 2012; Correa-Mora et al., 2009; Guzmán-Speziale, 2001). This study reveals that there could be an important interaction between different faults of the ESFZ. This is evident in the Lempa and El Triunfo Faults detailed study, where there are deformation reliefs and an accommodation zone between them, interpreted from the results of the topography analysis (Fig. 9).

The Lempa inter-segment zone is the area where distributed deformation dominates, making this region an interesting zone for future seismic hazard studies because it may be an area acting as a seismic barrier or asperity in large earthquakes along the ESFZ.

The measure of the basin axes in the Berlin Segment area has been a useful tool in order to assess the strike-slip motion of El Triunfo Fault and its slip-rate. We have interpreted along-strike variations of the horizontal slip-rate from 4.6 mm/year to 1.0 mm/year decreasing approximately from the center towards the tips of the fault. From the hypsometric analysis, we have interpreted variations along-strike in the dip-slip movement of the fault, being the maximum uplift in the middle and the lowest in the tips. The behavior of the El Triunfo Fault presents a classical bell shaped distribution of the slip along the fault.

The hypsometric curves and hypsometric integrals of the basins of the San Vicente segment and the geomorphological expression of this fault can be explained by the hypothesis of a reactivation of structures

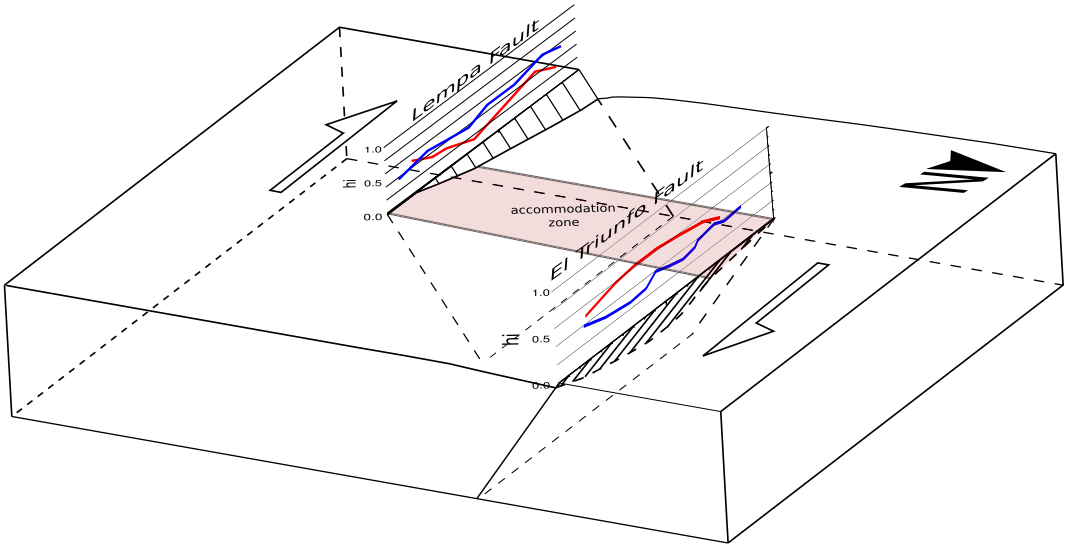

Fig. 9. Interpreted structure of Lempa and El Triunfo Faults. Diagrams are profiles 7B and 7C.

inherited from the previous extensional tectonic regime and a recent rotation in the maximum shortening direction. A similar tectonic evolution as described by Weinberg (1992) in Nicaragua is possible and could explain the anomalous results in the hypsometric analyses of the San Vicente fault linked to a very high scarp.

Acknowledgments

This research has been supported by the project "GEOTÁCTICA" Analysis of the active tectonics and volcano–tectonic interactions in El Salvador using geological, geotechnical and geophysical data. Ref.: CGL2009-14405-C02-02. We are grateful to our colleagues at DGOA-MARN (Observatorio Ambiental): Manuel Díaz and Douglas Hernández for their assistance. The first author acknowledges financial support for this publication provided by a pre-doctoral grant of the International Campus Excellence of Madrid (UCM–UPM), Spain. Some figures were produced using GMT software (Wessel and Smith, 1991). We also thank to the Editor Mian Liu and two anonymous reviewers their constructive comments that improved the original manuscript.

References

Agostini, S., Corti, G., Doglioni, C., Carminati, E., Innocenti, F., Tonarini, S., Manetti, P., Di Vincenzo, G., Montanari, D., 2006. Tectonic and magmatic evolution of the active volcanic front in El Salvador: insight into the Berlín and Ahuachapán geothermal areas. Geothermics 35 (4), 368–408.

Álvarez-Gómez, J.A., 2009. Tectónica activa y geodinámica en el norte de Centro América. PhD Thesis Dpt. Geodinamycs, Universidad Complutense de Madrid, Madrid.

Álvarez-Gómez, J.A., Meijer, P.T., Martínez-Díaz, J.J., Capote, R., 2008. Constraints from finite element modeling on the active tectonics of northern Central America and the Middle America Trench. Tectonics 27. http://dx.doi.org/10.1029/2007TC002162 (TC1008).

Authemayou, C., Brocard, G., Teyssier, C., Simon-Labric, T., Guttierrez, A., Chiquin, E.N., Moran, S., 2011. The Caribbean–North America–Cocos triple junction and the dynamics of the polochic–motagua fault systems: pull-up and zipper models. Tectonics 30 (30). http://dx.doi.org/10.1029/2010TC002814 (TC3010).

Bosse, H.R., Lorenz, W., Merino, A., Mihm, A., Rode, K., Schmidt-Thomé, M., Wiesemann, G., Weber, H.S., 1978. Geological map of El Salvador Republic: Hannover Germany. Bundesanstalt für Geowissenschaften und Rohstoffe, D-3 scale 1:100,000.

Burbank, D.W., Anderson, R.S., 2001. Tectonic Geomorphology. Berlin, Federal Republic of Germany (DEU). Blackwell Science, Oxford (247 pp.).

Cáceres, D., Monterroso, D., Tavakoli, B., 2005. Crustal deformation in northern Central America. Tectonophysics 404, 119–131.

Canora, C., Martínez-Díaz, J.J., Villamor, P., Berryman, K., Álvarez-Gómez, J.A., Pullinger, C., Capote, R., 2010. Geological and seismological analysis of the Mw 6.6 13th February 2001 El Salvador earthquake: evidence for surface rupture and implications for seismic hazard. Bull. Seismol. Soc. Am. 100 (6), 2873–2890.

Canora, C., Villamor, P., Martínez-Díaz, J.J., Berryman, K., Álvarez-Gómez, J.A., Capote, R., Hernández, W., 2012. Paleoseismic analisys of the San Vicente segment of the El Salvador Fault Zone, El Salvador, Central America. Geol. Acta 10, 103–123.

Canora, C., Martínez-Díaz, J.J., Villamor, P., Berryman, K., Álvarez-Gómez, J.A., Capote, R., Díaz, M., 2014. Structural Evolution of the El Salvador Fault Zone:. An Evolving Fault System within a Volcanic Arc. (in press).

Carr, M.J., 1976. Underthrusting and Quaternary faulting in northern Central America. Geol. Soc. Am. Bull. 87, 825–829.

Cheng, K., Hung, J., Chang, H., Tsai, H., Sung, Q., 2012. Scale independence of basin hypsometry and steady state topography. Geomorphology 171–172, 1–11.

Correa-Mora, F., DeMets, C., Alvarado, D., Turner, H.L., Mattioli, G., Hernández, D., Pullinger, C., Rodríguez, M., Tenorio, C., 2009. GPS-derived coupling estimates for Central America subduction zone and volcanic arc faults: El Salvador, Honduras and Nicaragua. Geophys. J. Int. 179 (3), 1279–1291.

Corti, G., Carminati, E., Mazzarini, F., Garcia, M.O., 2005. Active strike-slip faulting in El Salvador, Central America. Geology 33, 989–992.

Cowie, P.A., Roberts, G.P., 2001. Constraining slip rates and spacings for active normal faults. J. Struct. Geol. 23 (4), 1901–1915.

DeMets, C., Mattioli, G., Jansma, P., Rogers, R.D., Tenorio, C., Turner, H.L., 2007. Present motion and deformation of the Caribbean plate: constraints from new GPS geodetic measurements from Honduras and Nicaragua. Geologic and Tectonic Development of the Caribbean Plate in Northern Central America: GSA Special Paper. 428, pp. 21–36.

DeMets, C., Gordon, R.G., Argus, D.F., 2010. Geologically current plate motions. Geophys. J. Int. 181, 1–80.

Ferrill, D.A., Morris, A.P., 2001. Displacement gradient and deformation in normal fault systems. J. Struct. Geol. 23 (4), 619–638.

Franco, A., Lasserre, C., Lyon-Caen, H., Kostoglodov, V., Molina, E., Guzman-Speziale, M., Manea, V.C., 2012. Fault kinematics in northern central america and coupling along the subduction interface of the cocos plate, from GPS data in Chiapas (Mexico), Guatemala and El Salvador. Geophys. J. Int. 189 (3), 1223–1236.

Funk, J., Mann, P., McIntosh, K., Stephens, J., 2009. Cenozoic tectonics of the Nicaraguan depression, Nicaragua, and Median Trough, El Salvador, based on seismic reflection profiling and remote-sensing data. Geol. Soc. Am. Bull. 121 (11/12), 1491–1521.

Guzmán-Speziale, M., 2001. Active seismic deformation in the grabens of northern Central America and its relationship to the relative motion of the North America–Caribbean plate boundary. Tectonophysics 337, 39–51.

Guzman-Speziale, M., Meneses-Rocha, J., 2000. The North America–Caribbean plate boundary west of the Motagua–Polochic fault system; a fault job in southeastern Mexico. J. S. Am. Earth Sci. 13 (4–5), 459–468.

Guzman-Speziale, M., Pennington, W.D., Matumoto, T., 1989. The triple junction of the North America, Cocos, and Caribbean plates; seismicity and tectonics. Tectonics 8 (5), 981–997.

Hare, P.W., Gardner, T.W., 1985. Geomorphic indicators of vertical neotectonism along converging plate margins, Nicoya Peninsula, Costa Rica. Binghamton Symposia in Geomorphology: International Series. 15, pp. 75–104.

Hart, W.J.E., 1981. The Panchimalco Tephra, El Salvador, Central America. MS thesis Rutgers University, New Brunswick, New Jersey 101.

Hart, W.J.E., 1983. Classic to Postclassic tephra layers exposed in archeological sites, eastern Zapotitan valley. In: Sheets, P.D. (Ed.), The Zapotitán Valley of El Salvador: Archeology and Volcanism in Central America. Univ Texas Press.

Keller, E.A., Pinter, N., 2002. Active Tectonics; Earthquakes, Uplift, and Landscape. Upper Saddle River, NJ, United States (USA). Prentice Hall, New Jersey (362 pp.).

Lyon-Caen, H., Barrier, E., Lasserre, C., Franco, A., Arzu, I., Chiquin, L., Chiquin, M., Duquesnoy, T., Flores, O., Galicia, O., Luna, J., Molina, E., Porras, O., Requena, J.,

Robles, V., Romeri, J., Wolf, R., 2006. Kinematics of the North American–Caribbean–Cocos plates in central america from new GPS measurements across the Polochic–Motagua fault system. Geophys. Res. Lett. 33 (19) (0-L19309).
Martinez-Diaz, J., Alvarez-Gomez, J., Benito, B., Hernandez, D., 2004. Triggering of destructive earthquakes in El Salvador. Geology 32 (1), 65–68.
McBirney, A.R., Williams, H., 1965. Volcanic history of Nicaragua. Publications in Geological Sciences. 55. University of California, p. 73.
Morell, K.D., Kirby, E., Fisher, D.M., van Soest, M., 2012. Geomorphic and exhumational response of the Central American Volcanic Arc to Cocos Ridge subduction. J. Geophys. Res. 117. http://dx.doi.org/10.1029/2011JB008969 (B04409).
Perez-Peña, J.V., Azor, A., Azanon, J.M., Keller, E.A., 2010. Active tectonics in the Sierra Nevada (Betic Cordillera, SE Spain); insights from geomorphic indexes and drainage pattern analysis. Geomorphology 119 (1–2), 74–87.
Pike, R.J., Wilson, S.E., 1971. Elevation-relief ratio, hypsometric integral, and geomorphic area-altitude analysis. Geol. Soc. Am. Bull. 82 (4), 1079–1083.
Plafker, G., 1976. Tectonic aspects of the Guatemala earthquake of 4 February 1976. Science 193 (4259), 1201–1208.
Rogers, R.D., Karason, H., van der Hilst, R.D., 2002. Epeirogenic uplift above a detached slab in northern Central America. Geology 30, 1031–1034.
Ruano, P., Rubí, C., Masana, E., Ortuño, M., Piqué, O., Santanach, P., 2008. Paleoseismology along the Cofradía fault. Managua, Nicaragua: Preliminary Results. 10. Geotemas.
Scholz, C.H., 2002. The Mechanics of Earthquake and Faulting, 2nd edition. Cambridge University Press, Cambridge, New York, Melbourne (447 pp.).
Strahler, A.N., 1952. Hypsometric (area-altitude curve) analysis of erosional topography. Geol. Soc. Am. Bull. 63 (11), 1117–1141.
van Wik de Vries, B., 1993. Tectonics and Magma Evolution of Nicaraguan Volcanic Systems. PhD Thesis Open University, Milton Keynes, UK.
Walcott, R.C., Summerfield, M.A., 2008. Scale dependence of hypsometric integrals; an analysis of southeast african basins. Geomorphology 96 (1–2), 174–186.
Walsh, J.J., Watterson, J., 1989. Displacement gradients on fault surfaces. J. Struct. Geol. 11 (3), 307–316.
Weinberg, R.E., 1992. Neotectonic development of western Nicaragua. Tectonics 11 (5), 1010–1017.
Wessel, P., Smith, W.H.P., 1991. Free software help maps and display data. EOS Trans. Am. Geophys. Union 72, 441–446.